

The Influence of Size on Phase Morphology and Li-Ion Mobility in Nanosized Lithiated Anatase TiO₂

Marnix Wagemaker,^{*[a]} Wouter J. H. Borghols,^[a] Ernst R. H. van Eck,^[b]
Arno P. M. Kentgens,^[b] Gordon J. Kearley,^[a] and Fokko M. Mulder^{*[a]}

Abstract: Sustainable energy storage in the form of Li-ion batteries requires new and advanced materials in particular with a higher power density. Nanostructuring appears to be a promising strategy, in which the higher power density in nanosized materials is related to the dramatically shortened Li-ion diffusion paths. However, nanosizing materials also changes intrinsic material properties, which influence both ionic and electronic conductivity. In this work neutron diffraction is used to show that in addition to these two aspects, nanostructuring changes the

phase behavior and morphology. Lithiated 40-nm TiO₂ anatase crystallites become single phase, either having the Li-poor original anatase phase, or the Li-rich Li-titanate phase, in contrast to microsized crystallites where these two phases coexist in equilibrium within one crystal particle. In addition, Li_xTiO₂ compositions occur with stoichiometries that are not stable in

Keywords: Li-ion battery • nanoionics • neutron diffraction • NMR spectroscopy • TiO₂ anatase

micron-sized crystallites, indicating enhanced solid solution behavior. Reduced conduction electron densities at the sites of the Li ions are observed by NMR spectroscopy. This is accompanied by reduced spontaneous Li-ion mobility, suggesting a correlation between the electron density at the Li-ion site and the Li-ion mobility. The present results show that in the case of lithiated anatase TiO₂, significant effects on phase composition, morphology, and electronic configurations are induced, as well as slower intracrystallite Li diffusion.

Introduction

The interest in the anatase phase of TiO₂ is attributed to its application as an electrode material in electrochromic devices^[1,2] and in Li-ion batteries.^[3–6] The latter application is related to the large number of Li ions that reversibly can be intercalated into the TiO₂ structure. Lithium insertion results in a phase transition from the original tetragonal (space group *I*₄/*amd*) anatase structure towards the orthorhombic Li_{x–0.5}TiO₂ phase, which we refer to as the Li-titanate phase (space group *Imma*).^[7] During intercalation of

microsized crystal particles, the two-phase equilibrium between these two phases is maintained by a continuous Li-ion exchange.^[8] The Li-ion storage capacity, and rate with which they can be inserted and extracted, depend strongly on the dimensions of the TiO₂ crystallites. In particular, nanostructured TiO₂ anatase appears to be interesting as it leads to strongly improved kinetic performance of the charge–discharge process. The better performance is the result of short, nanoscopic, through-particle diffusion paths, and in addition fast capacitor-like kinetics of surface-adsorbed Li on the particles may play a role. These effects can be observed for different anatase morphologies such as nanosheets,^[9] nanotubes^[10] and also for nanoporous anatase structures.^[6,11] Although nanosizing improves the overall kinetic performance of the material due to the increased surface area and shorter diffusion distances, the diffusion coefficient becomes smaller for smaller crystallite sizes. In single-crystal anatase, the chronoamperometric diffusion coefficient was found to be $D \approx 10^{-13} \text{ cm}^2 \text{ s}^{-1}$,^[12,13] whereas nanocrystalline anatase led to values between 10^{-17} and $10^{-14} \text{ cm}^2 \text{ s}^{-1}$.^[14–17] The decrease in diffusion coefficient with decreasing crystallite size has also been found for various other insertion compounds.^[18–20] The origin of the slower Li-ion transport to-

[a] Dr. M. Wagemaker, W. J. H. Borghols, Prof. Dr. G. J. Kearley, Dr. F. M. Mulder
Department of Radiation, Radionuclides and Reactors
Faculty of Applied Sciences, Delft University of Technology
Mekelweg 15, 2629 JB Delft (The Netherlands)
Fax: (+31) 152-788-303
E-mail: m.wagemaker@tnw.tudelft.nl
f.m.mulder@tnw.tudelft.nl

[b] Dr. E. R. H. van Eck, Prof. Dr. A. P. M. Kentgens
Department of Physical Chemistry - Solid State NMR, IMM
Radboud University Nijmegen
Toernooiveld 1, 6525 ED Nijmegen (The Netherlands)

wards or/and in nanocrystalline particles is not understood. Aspects that most likely influence the ionic- (and electronic-) conductivity in nanosized materials are defect concentrations and space-charges.^[21,22]

In this context, 40-nm TiO₂ anatase crystalline particles were chemically lithiated and investigated with neutron diffraction and NMR spectroscopy. Neutron diffraction (ND) is a sensitive probe for Li in this type of materials, while Li NMR spectroscopy provides a sensitive microscopic probe for both Li-ion dynamics and the local Li-ion environment. In previous investigations these methods were utilized to extract detailed structural and mobility information for Li intercalated in bulk, that is, microcrystalline, anatase.^[8,23,24] With this background it is possible to reveal fundamental differences between Li intercalation in nano- and microstructured anatase TiO₂. Such findings are likely to be more general for nanostructured Li intercalation compounds.

Results and Discussion

Neutron diffraction patterns for different overall compositions Li_xTiO₂ ($x=0, 0.12, 0.25, 0.55$) could be fitted in detail, as shown for $x=0.25$ in Figure 1. Similar to microsized crys-

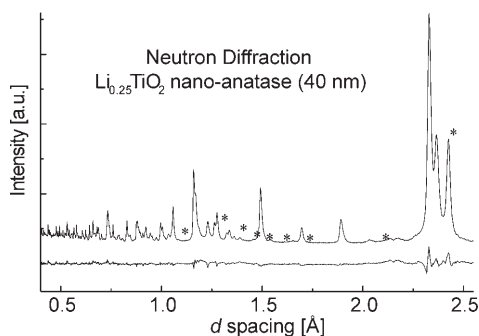


Figure 1. Neutron diffraction (TOF at $2\theta=91.38$ degree) pattern for Li_{0.25}TiO₂ including fit residual. Above d spacings of 1.0 Å, the positions of Li-titanate reflections are marked by asterisk. For this overall composition, 70% of the material has the original anatase phase and 30% the Li-titanate phase.

tallites, lithium insertion results in a gradual phase transition from the original tetragonal (space group $I4_1/amd$) anatase structure towards the orthorhombic Li-titanate phase (space group $Imma$).^[7] However, detailed fitting of the diffraction data reveals a number of essential differences. In Figure 2a, the domain sizes, deduced from the diffraction line-width, for both the anatase and Li-titanate phases are presented for different overall compositions.

The average size from transmission electron microscopy (TEM) for the initial TiO₂ anatase material (40 ± 3 nm) is consistent with the line-broadening observed from diffraction data. Remarkably, upon lithiation the line-width of both phases, anatase and Li-titanate, does not increase. Such broadening would be expected if both phases are present

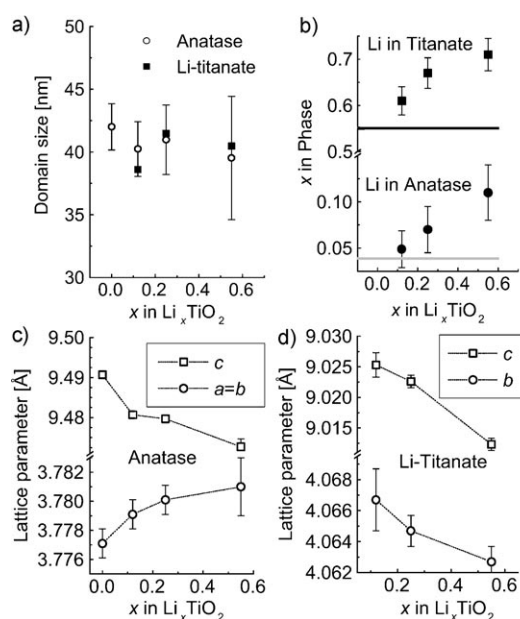


Figure 2. Neutron diffraction result for a) domain size from the diffraction line broadening for both phases (the error bars of the Li-titanate phase have the same order of magnitude as for the anatase phase, but have been left out for clarity of the figure) and b) result for the Li content in the anatase and the Li-titanate phase as a function of the overall composition. The top and bottom horizontal lines represent the result for the Li-titanate phase and the anatase phase in microsized powders, respectively. c) and d) Show the fitted lattice parameters for both phases as a function of the overall composition.

within one single crystal particle, since that would lead to anatase and Li-titanate crystal domains smaller than the initial single crystal particle, such as is observed for microsized lithiated TiO₂ anatase crystals.^[23] It can also be mentioned that coexistence of both phases within one particle would cause additional broadening of the Bragg reflections due to strain as a result of the volume difference between the two phases (~5%). The absence of any broadening implies that upon lithiation the size of the anatase and Li-titanate domains remain equal to the original single-crystal particle size, which can only mean that the nanoparticle is either Li-anatase or Li-titanate. The absence of reduced Bragg peak intensity and increased background indicates that the particles do not lose crystallinity upon lithiation. TEM experiments appeared unsuitable for the observation of the phase composition inside individual particles. The main reasons are: 1) while performing TEM we observed changes of the lithiated nanostructured material, indicating that the measurement itself was influencing the system, and 2) the lattice parameters between both phases are only slightly different (Li cannot be seen).

The absence of a two-phase equilibrium within nanosized crystallites was also suggested for 15-nm crystallite-sized mesoscopic material probed in situ with XRD.^[25] Apparently, the two-phase system is not stable within 40-nm single crystals, whereas it is stable in ~2 μm crystalline particles.^[25] In the micro-sized Li_xTiO₂ phase, the spontaneously formed domains, either with the anatase or with the Li-titanate

phase, are 60–100 nm in size.^[23] Such domain formation will result in an energy penalty due to the phase boundaries. The presence of the two-phase equilibrium in micro-sized crystallites implies that the free energy of the combination of the two phases, anatase Li_{0.026}TiO₂ and Li-titanate Li_{0.55}TiO₂, is lower than that of a solid solution, Li_xTiO₂, with the same overall composition. In other words, the combination of the two phases including the phase boundaries has a lower free energy than a solid solution (which has no phase boundaries). It seems that introduction of a phase boundary in 40-nm-sized TiO₂ crystallites leads to an energetically unfavorable situation, and the formation of either anatase or Li-titanate is more favorable, at least for the overwhelming majority of the particles as observed from the constant diffraction line width. The thermodynamic destabilisation of the two-phase equilibrium with decreasing crystallite sizes has also been predicted for binary mixtures.^[26]

Variation of the lattice parameters in both phases as a function of the overall composition (Figure 2c and d) indicates that the Li fraction in both phases is not constant. The ND fit results in Figure 2b confirm this suggestion. This finding is in sharp contrast to the microcrystalline material in which the intra-phase Li contents in the two coexisting phases are found to be constant for overall compositions up to $x=0.55$; in that case the phase fractions vary so as to keep the Li contents of the two different phases constant. Note that we use “overall composition” to indicate the average Li content in the whole material (which is a combination of the two phases, anatase and Li-titanate), in contrast to the local composition of an individual phase. For the nanomaterial the latter varies with overall composition, as illustrated by Figure 2b. In the Li-rich Li-titanate phase the local Li content increases up to 0.7 in the nanosized material, compared to 0.55 in the micro-sized material. The nanostructured anatase phase is able to host about 0.1 Li per Ti, which is considerably more than in micro-sized crystals (maximum of 0.026).^[23] The overall composition calculated from the phase fractions and site occupations is consistent with chemical analysis from wet chemical inductively coupled plasma spectroscopy (ICP) as can be seen in Table 1. We

Table 1. Overall Li fraction, x , in the 40-nm Li_xTiO₂ material, x is the fraction if all butyllithium would react with the TiO₂ material, $x_{\text{ND-fit}}$ is the overall Li fraction from neutron diffraction (resulting from the Li fraction in each phase and the relative phase fractions), and x_{ICP} is the overall Li fraction from ICP analysis.

x_{BuLi}	$x_{\text{ND-fit}}$	x_{ICP}
0.12	0.09 ± 0.02	0.11 ± 0.01
0.25	0.25 ± 0.03	0.25 ± 0.01
0.55	0.54 ± 0.03	0.55 ± 0.02

conclude that in the nanomaterial apparently either anatase or Li-titanate with a “within limits” adjustable Li fraction is formed and there is no intra-crystal two-phase equilibrium observed. This indicates a larger solid solution domain for the nanomaterial, which was indeed observed.^[27]

Interestingly, Sudant et al.^[27] did not observe the Li-titanate phase in materials lithiated up to $x=0.15$, which implies that the solid solution domain in anatase extended at least up to $x=0.15$, whereas it only extends up to about 0.1 in the present results. This is most likely related to the crystallite size, Sudant et al. used approximately 6-nm crystallites compared to the 40-nm crystallites used in the present study. This suggests that the solid solution domain increases with decreasing particle size.

In Figure 3 ⁷Li MAS NMR spectra are shown (only the center-band) for three nanostructured samples with different

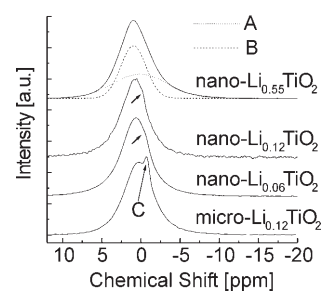


Figure 3. ⁷Li MAS NMR spectra of three nanostructured samples with indicated overall compositions and one microscopic composition for comparison. For micro-Li_{0.12}TiO₂, the small narrow resonance represents Li in the anatase phase (species C). For nano-Li_{0.06}TiO₂ and of nano-Li_{0.12}TiO₂, the arrows indicate the weak shoulder representing Li in the anatase phase, which is more visible for the micro-sized sample. The fit of nano-Li_{0.55}TiO₂ indicates the presence of species A (narrow) and B (broad) in the Li-titanate phase.

overall Li content. A spectrum of microcrystalline material is also added for comparison.^[24] For overall compositions in the range $0.026 < x < 0.55$ two phases coexist in microcrystalline particles,^[24] the Li-poor original anatase phase and the Li-rich Li-titanate phase. In microcrystalline particles, resonance C (see Figure 3) was assigned as Li in the original anatase phase (composition Li _{$x-0.026$} TiO₂).^[24] For the overall composition Li_{0.12}TiO₂, see bottom spectrum in Figure 3, species C is clearly recognizable as a narrow resonance on top of the broader resonance A, which is attributed to the Li in the Li-titanate structure.^[24]

In contrast, the same overall composition of the nanomaterial leads to almost complete disappearance of the narrow signal of species C associated with Li in the anatase phase. At first, it was suspected that although in an inert atmosphere, the sample might nevertheless have degraded due to air or moisture, but visual inspection after the measurements revealed that the samples retained their initial characteristic blue color indicating that it was not degraded. Additionally, the experiments were fully reproducible for different sample batches.

Close inspection of the ⁷Li MAS NMR spectra, see arrows in Figure 3, reveals a weak shoulder indicating that species C, representing Li in the anatase phase, is also present in the 40-nm crystallites. Although the ⁷Li MAS NMR spectra seem to indicate the absence of significant amounts

of Li in the anatase phase, the results from neutron diffraction (Figure 2) show that there is in fact a significant fraction of Li in the anatase phase. For the overall composition $x=0.55$, the Li fraction in anatase is more than 0.1, which is four times more than in the micro-sized material where it was found to be about 0.026.^[23] In addition, the T_2 measurements (below) indicate that there are two contributions to the spectra with intensity ratios in agreement with the intraphase Li contents found in the neutron measurements. This leads to the conclusion that the shape of the anatase signal is less visible because of broadening, which is also suggested by the lower T_2 value (for micron-sized anatase, T_2 reaches values of several ms,^[24] while it stays below 0.5 ms for nano-anatase). For $\text{Li}_{0.55}\text{TiO}_2$ in both nano- and microcrystals next to resonance A, a broad resonance occurs, B (see Figure 3), which was assigned by Luca et al.^[28] as Li in the Li-titanate phase. The negative chemical shift of species B was explained by a weak coupling of Li to conduction electron density.

The Li-ion spontaneous mobility was probed with static ^7Li NMR T_2 relaxation measurements. With the onset of Li-ion motion there will be an increase of the T_2 relaxation time, an effect that is referred to as motional narrowing (it causes the actual resonance in the frequency domain to become narrower). In this way the T_2 relaxation time is a probe of the Li-ion mobility, and knowledge of T_2 versus temperature allows the determination of the (self) diffusion coefficient and its activation energy, quantifying the barrier and the time-scale for Li hopping through the TiO_2 host lattice.^[24,29] For compositions with a significant amount of Li in the original anatase phase (small x), the T_2 relaxation time of Li in the anatase phase and Li in the titanate phase differ significantly, allowing straightforward discrimination of the two. Figure 4a,b indicate that for $x=0.06$ the mobility of Li in the anatase and the titanate phase becomes detectable just below 300 K. The resulting energy barriers (Table 2) are comparable to those in the microcrystalline material, although the diffusion coefficients are smaller. However, for $x=0.12$ the situation has completely changed, the barrier in anatase being significantly lower, whereas Li in titanate appears to be frozen, at least up to the maximum temperature measured (413 K). Also for the overall composition $x=0.55$, Li in titanate appears to be frozen (not shown), the only difference is that the low temperature T_2 value is slightly larger, $T_2=52\ \mu\text{s}$. For the overall composition $x=0.55$, the Li in anatase signal is too weak to be deconvoluted due to the small amount of this phase.

The absence of a temperature dependence of T_2 for Li in the titanate phase at $x=0.12$ and $x=0.55$ prevents the determination of the diffusion coefficient and the barrier height for interstitial Li-ion diffusion. However, by assuming that the barrier height is at least the same as for $x=0.06$, and that the temperature dependence (motional narrowing) starts above the highest measured temperature, an approximate upper limit can be calculated for the diffusion coefficient at room temperature in Li-titanate. This value (Table 2) is significantly smaller than that for $x=0.06$, and

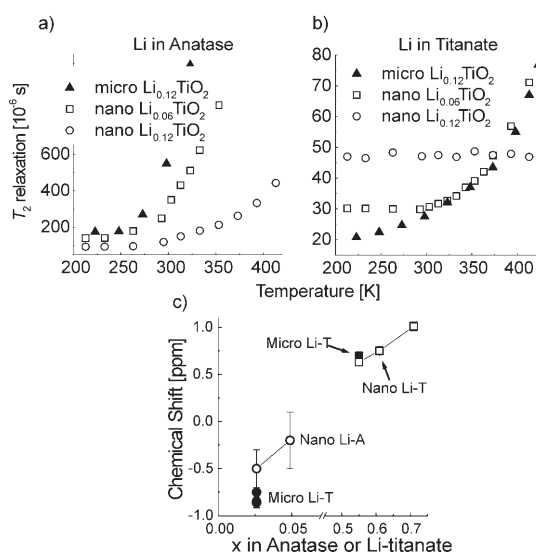


Figure 4. a, b) Variation of the ^7Li T_2 relaxation time with temperature for different nanostructured overall compositions, and one microstructured overall composition, inside the two phases (a) anatase and b) Li-titanate). The order of magnitude difference in T_2 between Li in anatase and titanate facilitates their accurate determination. c) ^7Li MAS chemical shift at room temperature in anatase and in Li-titanate for both nano- and micro-sized TiO_2 anatase crystals as a function of Li fraction in either the anatase or Li-titanate phase.

Table 2. Self diffusion coefficients and activation energies from T_2 NMR relaxation experiments in both phases present for three overall compositions of nanosized crystals, and for one overall composition of the micro-sized crystals as reported previously.^[24]

x	Particle	Phase	E_A [eV]	D_S [$10^{-12}\ \text{cm}^2\ \text{s}^{-1}$]
0.12	micro	anatase	0.2	4.7 ($T=293\ \text{K}$)
0.12	micro	Li-titanate	0.09	13 ($T=293\ \text{K}$)
0.06	nano	anatase	0.19	1.9 ($T=293\ \text{K}$)
0.06	nano	Li-titanate	0.16	5.7 ($T=293\ \text{K}$)
0.12	nano	anatase	0.16	1.1 ($T=293\ \text{K}$)
0.12	nano	Li-titanate	–	< 4.9 ($T=413\ \text{K}$), ~1.8 ($T=293\ \text{K}$)
0.55	nano	Li-titanate	–	< 4.6 ($T=413\ \text{K}$), ~1.7 ($T=293\ \text{K}$)

almost a factor of 10 smaller than the diffusion coefficient for Li in Li-titanate in micro-sized crystalline particles. In addition to the structural differences of both phases, anatase and Li-titanate, for different overall compositions (see Figure 2), also the Li-ion mobility significantly changes. Although care should be taken by comparing self-diffusion coefficients with chemical diffusion coefficients, the observed decrease in the (self-) diffusion coefficient for nanomaterials compared to micro-sized materials is consistent with what has been observed with macroscopic electrochemical measurements.^[12–17] These results actually show that the observed decrease in chemical diffusion coefficient is most likely due to decreased Li-ion bulk mobility, as opposed to a surface effect. The present results reveal that the reduced mobility appears to be an indirect consequence of the crystallite size. The small particle size causes the formation of either anatase or Li-titanate with a “within limits” adjustable Li fraction, which can be expected to influence the Li-ion mobility.

An interesting observation is that the static (low temperature) T_2 value for Li in titanate increases with x , from $T_2 = 30 \mu\text{s}$ for $x = 0.06$ up to $T_2 = 52 \mu\text{s}$ for $x = 0.55$. This increase corroborates the observation that the local Li environment in the Li-titanate nanocrystallites changes with changing overall composition (see Figure 2 b and d). In contrast, the Li environment and T_2 in the two well-defined coexisting phases in micro-sized lithiated TiO₂ do not vary with overall composition.

The change in local Li environment in the nanomaterial is also observed in the chemical shift dependence on the intra-phase composition shown in Figure 4c, while for the micro-sized material such a dependence on the composition is absent. A number of publications have illustrated that the Li-ion chemical shift in anatase Li_{*x*}TiO₂, and also in spinel Li_{1+*x*}Ti_{2-*x*}O₄, appears to be a probe of the conduction electron density at the ⁷Li nuclear site, which induces a small Knight shift.^[24,28,30] In principle, the applied static field induces a polarization that enhances the field locally at the Li-ion nucleus. In these materials the polarization lowers the chemical shift, which is explained by polarization of the Li-2s electrons by the Ti-3d and O-2p electron density.^[24,30] Summarizing, one could say that the coupling with the conduction electrons appears to lead to a lower chemical shift.

Figure 4c shows the chemical shift versus the intra-phase composition in either the anatase or the Li-titanate phase for both the nano- and the micromaterial. As mentioned before, micromaterials with different overall compositions lead to the same intra-phase composition in the anatase and the Li-titanate phase. Consistently, the chemical shift of Li in both phases in micromaterials does not vary with the overall composition, which is confirmed by the overlapping points in Figure 4c. In contrast to that, neutron diffraction of the nanomaterial shows that the Li composition inside the two phases is not constant as a function of the overall composition (see Figure 2b). Compared to the micromaterial, the Li fraction is significantly increased in both phases of the nanomaterial which (see Figure 4c) results in an increase of the chemical shift in each of the two phases. Hence, we conclude that a higher Li fraction leads to a higher chemical shift.

Combining previous paragraphs, the higher chemical shift of Li for the nanosized compositions, which occurs for overall compositions $x > 0.06$, indicates less coupling with conduction electrons, or a decrease of the conduction electron density at the Fermi level when compared to the micro-sized material. The exact nature of the reduced coupling and/or reduced conduction electron density at the Fermi level is unknown to the best of our knowledge and is part of our future research. This weaker interaction of Li ions with conduction electrons in the nanomaterial is an interesting observation, because a weaker interaction with the conduction electrons in the micromaterial was previously correlated with reduced Li-ion mobility.^[31] The conduction electron density at the Li-ion site was suggested to enhance the Li-ion mobility. A possible explanation for this is that a higher electron density partially screens the Li-ion, thereby reduc-

ing the barriers for diffusion (such an effect was also observed in LiMn₂O₄ above the charge ordering temperature^[32]). In this context the reduced Li-ion mobility in the Li-titanate phase in the nanosized material is consistent with its chemical shift being more positive, indicating a lower local electron density. In other words, the coupling between the conduction electrons and the Li ions might influence the Li-ion mobility (as in reference [24]), and could explain the reduced Li-ion mobility in nanomaterials. However, also the change in Li composition in each phase could cause a change in mobility.

Conclusion

Neutron diffraction and solid-state NMR reveal significant differences between micron- and nanostructured anatase TiO₂ upon intercalation. The ND data shows that in lithiated nanosized anatase TiO₂, crystal particles have either the original anatase phase, or the Li-titanate phase, where a relatively high Li occupancy is present in both phases. This is in contrast with micro-sized anatase TiO₂, where the two phases coexist within one crystallite maintaining an equilibrium and consequently constant Li fractions in both phases. The larger Li fractions are a likely source for the change in the local conduction electron density at the Fermi level, as is deduced by NMR spectroscopy. Direct measurement by NMR spectroscopy of the self-diffusion in both phases in the nanomaterial shows that the Li-mobility is strongly modified compared with that found for the micromaterial. The most striking difference is that Li appears to be frozen in the nanosized Li-titanate phase at high overall Li fractions. The altered electronic density at the Li site is correlated with the observed changes in the Li-ion mobility. These results show that in addition to defects and space charges, nanostructuring ionic materials has a surprising significant impact on Li intercalation behavior, capacity, Li-ion mobility, and phase morphology.

Experimental Section

Nanostructured TiO₂ anatase obtained from Altair (40 nm) was chemically lithiated with *n*-butyllithium^[33] and investigated with neutron diffraction (GEM, ISIS^[34]) and ⁷Li ($I = 3/2$, 92.6% abundance) NMR spectroscopy. The TiO₂ powder was mixed with hexane (anhydrous 95+%, Aldrich), and the *n*-butyllithium was added slowly while the mixture was stirred to guarantee homogeneous lithiation of the material. The advantage of using chemical intercalation, compared to electrochemical intercalation, is the amount of material that can be produced (in particular for neutron diffraction) in a clean way without electrolyte contamination of the powders. Because this work focuses on the behavior of Li ions within the TiO₂ anatase crystal matrix, the method by which Li was inserted (chemical or electrochemical) is not expected to influence the intrinsic properties of Li in TiO₂ anatase. The resulting overall chemical composition was checked independently using inductively coupled plasma (ICP) spectroscopy. Analysis of the neutron diffraction line broadening gives information on the crystallite size and strain. Since strain and crystal size have a different effect on the line shape, the two contributions to the line broadening can be distinguished. By fitting with a TOF peak shape in-

cluding both terms, quantitative data was obtained indicating that mainly crystallite broadening plays a role in these materials. Magic angle spinning (MAS) and static NMR spectra were recorded on a Chemagnetics 600 Infinity spectrometer ($B_0=14.1$ T) operating at 233.2 MHz. The MAS probe head with 3.2-mm airtight zirconia rotors achieved spinning speeds up to 19.2 kHz in a dry nitrogen atmosphere. Chemical shifts were referenced to a 0.1 M LiCl aqueous solution. The spectra were recorded after a 30° (at $2\nu_1$, with $\nu_1=89$ kHz) radio frequency pulse applied with a recycle delay of 20 s to ensure quantitative measurement conditions. The T_1 relaxation time was determined to be well below 5 s for all temperatures using a saturation recovery experiment. Neutron diffraction (ND) is a sensitive probe for Li in this type of materials, while ^7Li NMR spectroscopy provides a sensitive microscopic probe for both Li-ion dynamics and the local Li-ion environment. Although ^6Li NMR spectroscopy provides better resolution, ^7Li NMR spectroscopy is preferred in this case as it allows the Li-ion dynamics to be probed via the larger nuclear spin of ^7Li which leads to larger dipolar broadening. Additionally, it provides better comparison to previously published results on microsized crystal particles where ^7Li NMR spectroscopy was successfully applied to elucidate detailed properties of lithiated TiO_2 anatase.^[8,24]

Acknowledgements

This work is a contribution from the Delft Institute for Sustainable Energy (DISE). Financial support from the Netherlands Organization for Scientific Research (NWO), for VENI grant of M.W. and neutron beam time at ISIS, is gratefully acknowledged. We thank Laurent Chapon for assistance with the neutron diffraction measurements at GEM (ISIS) and Ugo Lafont for performing TEM measurements.

- [1] T. Ohzuku, T. Hirai, *Electrochim. Acta* **1982**, 27, 1263.
- [2] C. Bechinger, S. Ferrer, A. Zaban, J. Sprague, B. A. Gregg, *Nature* **1996**, 383, 608.
- [3] F. Bonino, L. Busani, M. Lazzari, M. Manstretta, B. Rivolta, B. Scrosati, *J. Power Sources* **1981**, 6, 261.
- [4] S. Y. Huang, L. Kavan, I. Exnar, M. Gratzel, *J. Electrochem. Soc.* **1995**, 142, L142.
- [5] T. Ohzuku, Z. Takehara, S. Yoshizawa, *Electrochim. Acta* **1979**, 24, 219.
- [6] H. S. Zhou, D. L. Li, M. Hibino, I. Honma, *Angew. Chem.* **2005**, 117, 807; *Angew. Chem. Int. Ed.* **2005**, 44, 797.
- [7] R. J. Cava, D. W. Murphy, S. Zahurak, A. Santoro, R. S. Roth, *J. Solid State Chem.* **1984**, 53, 64.
- [8] M. Wagemaker, A. P. M. Kentgens, F. M. Mulder, *Nature* **2002**, 418, 397.
- [9] L. Kavan, M. Kalbac, M. Zukulova, I. Exnar, V. Lorenzen, R. Nesper, M. Gratzel, *Chem. Mater.* **2004**, 16, 477.
- [10] X. P. Gao, H. Y. Zhu, G. L. Pan, S. H. Ye, Y. Lan, F. Wu, D. Y. Song, *J. Phys. Chem. B* **2004**, 108, 2868.
- [11] H. Yamada, T. Yamato, I. Moriguchi, T. Kudo, *Chem. Lett.* **2004**, 33, 1548.
- [12] L. Kavan, M. Gratzel, S. E. Gilbert, C. Klemenz, H. J. Scheel, *J. Am. Chem. Soc.* **1996**, 118, 6716.
- [13] R. Hengerer, L. Kavan, P. Krtil, M. Gratzel, *J. Electrochem. Soc.* **2000**, 147, 1467.
- [14] L. Kavan, J. Rathousky, M. Gratzel, V. Shklover, A. Zukal, *J. Phys. Chem. B* **2000**, 104, 12012.
- [15] M. P. Cantao, J. I. Cisneros, R. M. Torresi, *J. Phys. Chem.* **1994**, 98, 4865.
- [16] H. Lindstrom, S. Sodergren, A. Solbrand, H. Rensmo, J. Hjelm, A. Hagfeldt, S. E. Lindquist, *J. Phys. Chem. B* **1997**, 101, 7710.
- [17] R. van de Krol, A. Goossens, J. Schoonman, *J. Phys. Chem. B* **1999**, 103, 7151.
- [18] Y. M. Choi, S. I. Pyun, *Solid State Ionics* **1997**, 99, 173.
- [19] M. D. Levi, D. Aurbach, *Electrochim. Acta* **1999**, 45, 167.
- [20] L. Kavan, J. Prochazka, T. M. Spilner, M. Kalbac, M. T. Zukulova, T. Drezen, M. Gratzel, *J. Electrochem. Soc.* **2003**, 150, A1000.
- [21] N. Sata, K. Eberman, K. Eberl, J. Maier, *Nature* **2000**, 408, 946.
- [22] J. Maier, *Solid State Ionics* **2003**, 157, 327.
- [23] M. Wagemaker, G. J. Kearley, A. A. van Well, H. Mutka, F. M. Mulder, *J. Am. Chem. Soc.* **2003**, 125, 840.
- [24] M. Wagemaker, R. van de Krol, A. P. M. Kentgens, A. A. van Well, F. M. Mulder, *J. Am. Chem. Soc.* **2001**, 123, 11454.
- [25] R. van de Krol, A. Goossens, E. A. Meulenkaamp, *J. Electrochem. Soc.* **1999**, 146, 3150.
- [26] W. C. Johnson, *Acta Materialia* **2001**, 49, 3463.
- [27] G. Sudant, E. Baudrin, D. Larcher, J. M. Tarascon, *J. Mater. Chem.* **2005**, 15, 1263.
- [28] V. Luca, T. L. Hanley, N. K. Roberts, R. F. Howe, *Chem. Mater.* **1999**, 11, 2089.
- [29] N. Bloembergen, E. M. Purcell, R. V. Pound, *Phys. Rev.* **1948**, 73, 679.
- [30] M. Dalton, D. P. Tunstall, J. Todd, S. Arumugam, P. P. Edwards, *J. Phys. Condens. Matter* **1994**, 6, 8859.
- [31] P. C. M. Gubbens, M. Wagemaker, S. Sakarya, M. Blaaauw, A. Yaouanc, P. D. de Reotier, S. P. Cottrell, *Solid State Ionics* **2006**, 177, 145.
- [32] V. W. J. Verhoeven, I. M. de Schepper, G. Nachtegaal, A. P. M. Kentgens, E. M. Kelder, J. Schoonman, F. M. Mulder, *Phys. Rev. Lett.* **2001**, 86, 4314.
- [33] M. S. Whittingham, M. B. Dines, *J. Electrochem. Soc.* **1977**, 124, 1387.
- [34] W. G. Williams, R. M. Ibberson, P. Day, J. E. Enderby, *Physica B+C* **1997**, 241, 234.

Received: June 8, 2006
Published online: December 11, 2006